ACS APPLIED MATERIALS & INTERFACES

Subscriber access provided by UNIV OF NEBRASKA - LINCOLN

Article

Tuning the Structural Color of a 2D Photonic Crystal using a Bowl-Like Nanostructure

Ha Nee Umh, Sungju Yu, Yong hwa Kim, Su Young Lee, and Jongheop Yi

ACS Appl. Mater. Interfaces, **Just Accepted Manuscript** • DOI: 10.1021/acsami.6b03717 • Publication Date (Web): 01 Jun 2016

Downloaded from http://pubs.acs.org on June 7, 2016

Just Accepted

"Just Accepted" manuscripts have been peer-reviewed and accepted for publication. They are posted online prior to technical editing, formatting for publication and author proofing. The American Chemical Society provides "Just Accepted" as a free service to the research community to expedite the dissemination of scientific material as soon as possible after acceptance. "Just Accepted" manuscripts appear in full in PDF format accompanied by an HTML abstract. "Just Accepted" manuscripts have been fully peer reviewed, but should not be considered the official version of record. They are accessible to all readers and citable by the Digital Object Identifier (DOI®). "Just Accepted" is an optional service offered to authors. Therefore, the "Just Accepted" Web site may not include all articles that will be published in the journal. After a manuscript is technically edited and formatted, it will be removed from the "Just Accepted" Web site and published as an ASAP article. Note that technical editing may introduce minor changes to the manuscript text and/or graphics which could affect content, and all legal disclaimers and ethical guidelines that apply to the journal pertain. ACS cannot be held responsible for errors or consequences arising from the use of information contained in these "Just Accepted" manuscripts.

ACS Publications

ACS Applied Materials & Interfaces is published by the American Chemical Society.
1155 Sixteenth Street N.W., Washington, DC 20036

Published by American Chemical Society. Copyright © American Chemical Society. However, no copyright claim is made to original U.S. Government works, or works produced by employees of any Commonwealth realm Crown government in the course of their duties.

Tuning the Structural Color of a 2D Photonic Crystal using a Bowl-Like Nanostructure

*Ha Nee Umh,‡ Sungju Yu,‡ Yong Hwa Kim, Su Young Lee, and Jongheop Yi**

World Class University Program of Chemical Convergence for Energy & Environment, School of Chemical and Biological Engineering, Institute of Chemical Processes, Seoul National University, Seoul 151-742, Republic of Korea.

*Corresponding E-mail: jyi@snu.ac.kr

KEYWORDS: bio-inspired, 2D nanostructures, photonic crystal, nanobowl array, TiO_2, color patterning

ABSTRACT

Structural colors of the ordered photonic nanostructures are widely used as an effective platform for manipulating the propagation of light. Although several approaches have been explored in attempts to mimic the structural colors, improving the reproducibility, mechanical stability, and the economic feasibility of sophisticated photonic crystals prepared by complicated processes continue to pose a challenge. In this study, we report on an alternative, simple method

for fabricating a tunable photonic crystal at room temperature. A bowl-like nanostructure of TiO_2 was periodically arranged on a thin Ti sheet through a two-step anodization process where its diameters were systemically controlled by changing the applied voltage. Consequently, they displayed a broad color distribution, ranging from red to indigo, and the principal reason for color generation followed the Bragg diffraction theory. This non-colorant method was capable of reproducing a Mondrian painting on a centimeter scale without the need to employ complex architectures, where the generated structural colors were highly stable under mechanical or chemical influence. Such a color printing technique represents a potentially promising platform for practical applications for anti-counterfeit trademarks, wearable sensors, and displays.

INTRODUCTION

The structural coloration arises from the interaction of light and periodically arranged nanostructures, a so-called photonic crystal (PhC), which has drawn great interest in such diverse areas as Bragg mirrors, displays, colorimetric sensors and coloration of metal surface due to their fascinating properties.[1-6] Coloration in the PhCs is similar to mechanism of the color strategy in peacock feathers or wings of butterfly. Partial polarizations of 2D photonic bandgap (PBG) improve the interaction of light with matter, thereby inducing a color production.[7] Structural color has an origin in geometric structures, which differ from the most common color generation associated with the use of pigments or dyes. Compared to pigment-derived colors, structural color is usually iridescent, stable, and becomes brightened under sunlight.[8,9] In particular, the position of a stop-band can be modulated by tuning the refractive index and/or the periodicity of the PhC structure.[1-6,10,11]

PhCs with different stop-band energies have been generated by several approaches, including colloidal self-assembly,[12,13] lithography of metal films,[14,15] and direct laser writing.[16,17] However,

these methods involve some factors that need to be overcome, such as sacrificial templates, complicated fabrication process, and difficulties associated with large scale production and integration for producing reported-PhCs in spite of high resolution. Recently, metal plate anodization technique has been reported as a simple and scalable route to the preparation of high-quality arrays of nanostrucutres.[18-20] For instance, the anodization method has been widely used to fabricate nanoporous structures of Al_2O_3 and Si materials as it is cheap and offers high controllability over the process and convenience.[21-23] However, these metal colorations showed limitations that achromatic colors represented only in gray scale due to a low refractive index of Al_2O_3 and pore diameters was difficult to be controlled via HF etching.[21,23]

In this study, we report on a facile method for the design and construction of TiO_2 nanobowl arrays with a tunable structural color through the periodic modulation of the diameter of air cavities. Unlike other metal colorations, TiO_2 material not only displays full visible region but also extends application areas into gas-sensors,[24,25] photocatalysis,[26-29] and photovoltaics operating in visible light region.[30-32] For these reasons, TiO_2 was adopted in this work for applications in a wide variety of research fields. TiO_2 nanobowl arrays were prepared by a two-step anodization method where the diameter of the cavities was engineered by altering the anodization voltage used in the process. The resulting TiO_2 PhCs, which were composed of regularly arranged shallow bowls in the wavelength scale of light, created two different reflection peaks from the flat bottoms and inclined planes of the cavities. These reflections lead to color mixing, which is then visually detectable. The photonic band became red-shifted when the diameter of the air cavities was increased from 41 to 106 nm and thus generating a vivid rainbow color.

The realized colors were predictable according to Bragg diffraction theory, and were dependent only on the lattice spacing. Finally, a Mondrian painting was successfully printed on a 10 cm × 8 cm Ti foil without any complex architectures, showing a high resolution and stability when the specimen was exposed, even to strong UV light and toxic solvents. This strategy can eliminate the barriers posed by previous approaches and makes it possible to easily tune the reflected wavelength showing bi-structural colors within a short time.

EXPERIMENTAL SECTION

Fabrication of TiO_2 Nanobowl Arrays. A high-purity Ti foil (99.7%, 0.127 mm thickness, Sigma-Aldrich) was cut into 1 cm × 4 cm sections. The Ti sheets were degreased by sonicating in acetone, ethanol, and deionized water (DI water) in sequence. A Ti sheet was used as an anode with a Pt mesh as a cathode in a two-electrode system where the electrolyte consisted of 97 vol% of ethylene glycol (99.9%, Samchun), 3 vol% DI water, and 0.3 wt % NH_4F (≥98.0 %, Sigma-Aldrich). The Ti sheet was first anodized using a variety of voltages (30, 40, 50, 60, 65, and 75 V) for 1 h using DC power supply (PAP-3001, Powertron). The oxidized layer was then completely removed by using a sticky tape and ultasonication. The second anodization was performed under the same conditions as the first anodizing process for 240 s (at 30 V), for 180 s (at 40 V), for 120 s (at 50 V), for 90 s (at 60 V), for 50 s (at 65 V), and for 40 s (at 75 V) to obtain more stable and uniform structure. The temperature was maintained at 15 °C by circulating a coolant through an external temperature-control device during the anodizing processes.

Color Printing. A Ti foil was cut into 10 cm × 8 cm sheets, and a sketch of the original painting was drawn on the Ti sheet. Before the anodizing step, all parts of the Ti sheet were coated with an insulating adhesive, nitrocellulose layer, except for the areas to be colored. The

layer acts as a protective coat which inhibits the infiltration of electrolyte. This makes it possible to achieve the selective anodization of uncoated sections. The exposed sections of the Ti sheet were first anodized at a certain voltage for 1 h, followed by the elimination of the oxidized layers, as described above. In turn, the neighboring sections were subjected to a second anodization at the same voltage for the corresponding time. And then, the coating layer was removed by acetone and water. The other colors were also printed on the Ti sheet in the same way.

Sample Characterization. The morphology and size of the resulting films were observed using a field emission scanning electron microscope (FE-SEM, Sigma, Carl Zeiss). The reflectance spectra were obtained by an ultraviolet-visible diffuse reflectance spectroscopy (UV-DRS, V670, Jasco).

RESULT AND DISCUSSION

The procedure for fabricating the TiO_2 nanobowl arrays is illustrated in Figures 1a–d. A thin Ti foil was first anodized at a certain potential in the range of 30–75 V to produce TiO_2 nanotubes with different diameters. The rough and irregular TiO_2 nanotubes were completely removed using a sticky tape and ultrasonication, leaving a hexagon-shaped concavity pattern on the surface of the Ti foil. The pretreated Ti foil was anodized a second time at the same potential applied as was used in the first anodization step for several seconds, consequently forming hierarchical TiO_2 nanobowl arrays. It should be noted that the imprinted pattern that remained after the first anodization plays a crucial role in determining the diameter of the nanobowls. TiO_2 nanobowl arrays were prepared a total of three times for checking the reproducibility of this process. Field emission scanning electron microscope (FESEM) images in Figures 2a–f, Figures S1a–f, and Figures S2a–f show the top view of the as-prepared TiO_2 nanobowl arrays, in which

the average diameter gradually increases from 41 nm to 106 nm with increasing applied potential: 30, 40, 50, 60, 65, and 75 V (Figures S3a–f).

The porous nanobowl arrays display structural color that strongly depends on the diameter of air cavity and thus shifts from indigo to red. The height of each TiO_2 nanobowl was around 100 nm in all of the arrays (Figures S4a–f). The thickness of the resulting TiO_2 nanobowl structures was sufficiently thin to generate light reflection from the bottom plane that served as a mirror layer in order to increase the scattering intensity of the normal incident light. However, if the height is too high, the film reflects white color due to multiple scattering.[33-35] That is, a thick PhC causes incoherent and multiple scattering of the incident light and then results in a low chroma of the structural color.

Figure 3 shows the measured optical reflection spectra where the as-synthesized TiO_2 nanobowl arrays exhibit two separated peaks; one narrow reflection peak and the other a broad reflection band. As the diameter of air cavity is increased from 41 to 106 nm, the two reflection peaks were linearly red-shifted and their full-width at half-maximum (FWHM) gradually increased. The measurements were also replicated a total of three times (Figures S5a–f). In particular, these characteristics were prominently featured in the broad reflection band as compared to a relatively narrow reflection peak, contributing to the interval between the two peaks to become wider. The corresponding optical image for each sample was given as the inset along with the reflection curve. The color gradually changed from indigo to red with increasing cavity diameter. Note that two different reflection peaks emanate from the flat bottoms and inclined planes of the cavity.[1,36,37] Lights reflected from the sides are visible to the bare eyes, while the reflection at the center or bottom is dissipated. Specifically, the incident light on the sides of the cavity is retro-reflected due to double reflection, and the polarization of the reflected

light is then rotated upon each reflection. These reflections lead to the color mixing, which thus are visible to the bare eyes. All of the reflection spectra were converted to CIE1931 chromaticity coordinates by UV/DRS (Figure S6), representing the color gamut of the method. It should be noted that this color shift allows one to print arbitrary features with complex and multiple length scales.

The structural color change of the TiO_2 nanobowl arrays was predictable through light diffraction and refraction theories, as schematically illustrated in **Scheme 1**. When light of a specific wavelength, λ, is incident on a regularly arranged structure with spacing d, the light is scattered along a lattice direction. If the scattered waves constructively interfere with each other, the path difference between the two waves is equal to an integer multiple of the radiation wavelength. Bragg's law derived from the constructive interference can be combined with Snell's law of refraction, and the resulting equation is given by,[38]

$$m\lambda = n_{\text{eff}} d(\sin\theta_{\text{i}} - \sin\theta_{\text{r}}) \quad (1)$$

where m is the order of diffraction, θ_{i} is the incident angle, θ_{r} is the reflected angle, and n_{eff} is the mean effective refractive index. The n_{eff} depends on the porous structure of the TiO_2 nanobowl arrays, and is defined as following equation,[39]

$$n_{\text{eff}} = \sqrt{f n_1^2 + (1-f) n_2^2} \quad (2)$$

where n_1 is 1 for the refractive index of the air, n_2 is 2.49 for the amorphous TiO_2, and f is the volume fraction of pore. The f can be determined from the d and wall thickness, w, of the TiO_2 nanobowl.[40]

$$f = 1 - \frac{2\pi w(w+d)}{\sqrt{3}(2w+d)^2} \quad (3)$$

If the incident light is directly reflected ($\theta_i = \theta_r$), this is called the *Littrow configuration*.[41-43] Equation (1) changes to,

$$m\lambda = 2d \cdot n_{eff} \sin\theta_r \quad (4)$$

This modified model can describe how the TiO_2 nanobowl arrays reflect light of certain wavelengths. It clearly indicates that the diameter of TiO_2 nanobowl arrays mainly to determine the structural color of this system. The reflected wavelengths can be calculated using the above equations, and the values with standard deviations are summarized with the associated parameters in **Table 1**. The calculated wavelengths, λ_c, also gradually increase with increasing cavity diameter, and the values were consistent with the experimentally reflected wavelengths. Although there are two variables, namely, the diameter and refractive index that can change the reflected wavelength, a change in diameter has much more influence on the reflectance of the PhCs than the refractive index.[6,44]

Color printing applying a structural color on a thin metal substrate has a high resistance to bleaching by sunlight and toxic solvents as compared to conventional methods for color generation using pigments or dyes.[45,46] Plasmonic materials can be used for color printing, based on surface plasmon resonances resulting from the oscillation of electrons between metal and dielectric interfaces.[47,48] However, producing patterns using photonic crystals or plasmonic materials with distinct colors remains a challenge because low reflectivity and diffraction-limitations are drawbacks to plasmonic color system. In order to enhance the reflectivity, a metal film or a metal oxide film can be used to obtain high reflectivity as spacer layer leading to an

increase in the cost and process step. The fabrication method introduced in this study was extended to a centimeter scale through a facile, quick, and cost-effective process. We reproduced a Mondrian painting known as *Composition with Color Planes and Gray Lines* on a 10 cm × 8 cm Ti sheet of without any complex architectures. Each color in the original painting shown in Figure 4a was produced by hierarchical arrays of the bowl structure with different diameters which were systemically designed from the modified Bragg's equation instead of a trial-and-error method for the production of the desired colors. Consequently, they display a similarity to the original colors, and the distinct colors showed a fine contrast and brightness in the reproduced painting (Figure 4b). This result suggests that the anodization method for a color printing can be a promising method to produce structural colors. The corresponding nanostructure for each color was further highlighted in a high magnification image of some selected areas (Figures 4c–f), which illustrated different diameters and a uniform alignment of the nanobowls.

The fabrication process allows a flexible design of printed images on a thin metal sheet and the colors are chemically/mechanically stable in a harsh environment for a long time, unlike chemical dyes or 3D photonic crystals. A peel test was performed on the TiO_2 nanobowl arrays to examine the mechanical stability of the nanostructure by attaching and detaching a section of Scotch tape over the film where the tape has an adhesive strength to metal of 2.5 N/cm (Figure S7). The findings indicated that the TiO_2 nanobowl arrays not only maintained their distinct colors and the nanostructure was preserved even under repetitive testing. The stability of structural color of the TiO_2 nanobowl arrays was compared with a conventional pigment-derived color under the irradiation of lights. The structural color was well maintained under the irradiation by direct sunlight or fluorescent light (Figure 5a), while a N3 dye, a standard

ruthenium-complex dye for dye-sensitized solar cells, was not stable on the commercial TiO_2 nanoparticles, P25, due to the oxidative degradation of the dye (Figures 5b,c). The fluorescent light contains a negligible UV, indicating that N3 dye does not undergo photocatalytic degradation by the excitation of P25 with a wide bandgap. The wavelength shift for the N3 absorption is caused by molecular deformation through a photosensitization process. In addition, when the TiO_2 nanobowl arrays were immersed in various solvents such as NaCl, HNO_3, NaOH, ethanol, acetone, benzene, and toluene, respectively, they remained stable. Figure S8 shows the stability of TiO_2 nanobowl arrays after being exposed to diverse stimulus. Although the refractive index is a variable that can cause a change in the reflected wavelength, the relative change in diameter is usually much more significant than the refractive index.[6,44] This method has great promise for practical applications including producing anti-counterfeit tags, wearable sensors, and displays. This system can be also combined with noble metal clusters or photoactive molecules for the photoelectrochemical conversion of hydrocarbons or producing H_2 from water.

CONCLUSIONS

In summary, a facile and cost-effective method for generating and tuning structural colors of a 2D photonic crystal on a Ti sheet is described. Hierarchical TiO_2 nanobowl arrays were fabricated by a two-step anodization process where the nanobowl structure brought about two different reflection peaks from its flat bottom and inclined plane. The positions of the two reflection peaks as well as their wavelength gap can be simply adjusted by changing the diameter of TiO_2 nanobowls that are dependent on the anodizing potential. The reflected wavelength gradually increased with changing the periodicity of the TiO_2 nanobowl, as expected from Bragg diffraction theory. This method enabled a broad color distribution with a high contrast and brightness to be created without employing complicated color generation. In addition, the

structural colors were easily realized on a centimeter scale and were highly stable to mechanical and chemical stress. We believe that this printing technique has such strong features as follows: (1) Realization of a broad color distribution and facile tuning of the structural color, (2) low cost for replicating images, (3) large-scale production of photonic crystals on thin and flexible substrates, and (4) chemical and mechanical stability. These properties are suited for practical applications, such as prints that cannot be forgee and security.

SUPPORTING INFORMATION

Supplementary data for reproducibility of TiO_2 nanobowl arrays, size distribution histograms, side-view images observed by FE-SEM, the CIE 1931 diagram, and the mechanical and chemical stability test results of TiO_2 nanobowl arrays. This information is available free of charge via the Internet at http://pubs.acs.org/.

ACKNOWLEDGEMENT

This research was supported by the Global Frontier R&D Program on Center for Multiscale Energy System funded by the National Research Foundation under the Ministry of Science, ICT & Future, Korea (NRF-2011-0031571), and Supercomputing Center/Korea Institute of Science and Technology Information with supercomputing resources including technical support (KSC-2015-C2-028).

AUTHOR CONTRIBUTIONS

‡These authors contribute equally to this work. J. Yi supervised this project, experiments, and manuscript writing. H. N. Umh and S. Yu designed the experiments, characterized the materials and wrote the manuscript. Y. H. Kim fabricated the materials. S. Y. Lee contributed to reflectance measurement. All the authors discussed the results and commented on this study.

REFERENCES

(1) Diao, Y. Y.; Liu, X. Y.; Toh, G. W.; Shi, L.; Zi, J. Multiple Structural Coloring of Silk-Fibroin Photonic Crystals and Humidity-Responsive Color Sensing. *Adv. Funct. Mater.* **2013**, *23*, 5373–5380.

(2) Arsenault, C.; Puzzo, D. P.; Manners. I.; Ozin. G. A. Photonic-Crystal Full Color Displays. *Nat. Photonics* **2007**, *1*, 468–472.

(3) Walia, J.; Dhindsa, N. Khorasaninejad, M; Saini, S. S. Color Generation and Refractive Index Sensing using Diffraction from 2D Silicon Nanowire Arrays. *Small* **2014**, *10*, 144–151.

(4) Fenzl, C.; Hirsch, T.; Wolfbeis, O. S. Photonic Crystals for Chemical Sensing and Biosensing. *Angew. Chem., Int. Ed.* **2014**, *53*, 3318–3335.

(5) Kumar, K.; Duan, H.; Hegde, R. S.; Koh, S. C. W.; Wei, J. N.; Yang, J. K. W. Printing Colour at the Optical Diffraction Limit. *Nat. Nanotechnol.* **2012**, *7*, 557–561.

(6) Kim, H.; Ge, J.; Kim, J.; Choi, S.-E.; Lee, H.; Lee, H.; Park, W.; Yin, Y.; Kwon, S. Structural Colour Printing using a Magnetically Tunable and Lithographically Fixable Photonic Crystal. *Nat. Photonics* **2009**, *3*, 534–540.

(7) Zi, J.; Yu, X.; Li, Y.; Hu, X.; Xu, C.; Wang, X.; Liu, X.; Fu, R. Coloration Strategies in Peacock Feathers. *Proc. Natl. Acad. Sci. U. S. A*. **2003**, *100*, 12576–12578.

(8) Potyrailo, R. A.; Ghiradella, H.; Vertiatchikh, A.; Dovidenko, K.; Cournoyer, J. R.; Olson, E. Morpho Butterfly Wing Scales Demonstrate Highly Selective Vapour Response. *Nat. Photonics* **2007**, *1*, 123–128.

(9) Bai, L.; Xie, Z,; Wang, W.; Yuan, C.; Zhao, Y.; Mu, Z.; Zhong, Q.; Gu, Z. Bio-Inspired Vapor-Responsive Colloidal Photonic Crystal Patterns by Inkjet Printing. *ACS Nano* **2014**, *8*, 11094–11100.

(10) Waterhouse, G. I. N.; Wahab, A. K.; Al-Oufi, M.; Jovic, V.; Anjum, D. H.; Sun-Waterhouse, D.; Llorca, j.; Idriss, H. Hydrogen Production by Tuning the Photonic Band Gap with the Electronic Band Gap of TiO_2. *Sci. Rep.* **2013**, *3*, 2849.

(11) Schaffner, M.; England, G.; Kolle, M.; Aizenberg, J.; Vogel, N. Combining Bottom-Up Self-Assembly with Top-Down Microfabrication to Create Hierarchical Inverse Opals with High Structural Order. *Small* **2015**, *11*, 4334–4340.

(12) Vogel, N.; Utech, S.; England, G. T.; Shirman, T.; Phillips, K. R.; Koay, N.; Burgess, I. B.; Kolle, M.; Weitz, D. A.; Aizenberg, J. Color from Hierarchy: Diverse Optical Properties of Micron-Sized Spherical Colloidal Assemblies. *Proc. Natl. Acad. Sci. U. S. A.* **2015**, *112*, 10845–10850.

(13) Chen, J. I. L.; Freymann, G. Von.; Choi, S. Y.; Kitaev, V.; Ozin, G. A. Amplified Photochemistry with Slow Photons. *Adv. Mater.* **2006**, *18*, 1915–1919.

(14) Cheng, F.; Gao, J.; Luk, T. S.; Yang, X. Structural Color Printing Based on Plasmonic Metasurfaces of Perfect Light Absorption. *Sci. Rep.* **2015**, *5*, 11045.

(15) Khorasaninejad, M.; Abedzadeh, N.; Walia, J.; Patchett, S.; Saini, S. S. Color Matrix Refractive Index Sensors Using Coupled Vertical Silicon Nanowire Arrays. *Nano Lett.* **2012**, *12*, 4228–4234.

(16) Radke, A.; Gissibl, T.; Klotzbücher, T.; Braun, P. V.; Giessen, H. Three-Dimensional Bichiral Plasmonic Crystals Fabricated by Direct Laser Writing and Electroless Silver Plating. *Adv. Mater.* **2011**, *23*, 3018–3021.

(17) Rill, M. S.; Plet, C.; Thiel, M.; Staude, I.; Freymann, G. Von; Linden, S.; Wegener, M. Photonic Metamaterials by Direct Laser Writing and Silver Chemical Vapour Deposition. *Nat. Mater*. **2008**, *7*, 543–546.

(18) Masuda, H.; Fukuda, K.; Ordered Metal Nanohole Arrays Made by a Two-Step Replication of Honeycomb Structures of Anodic Alumina. *Science* **1995**, *268*, 1466–1468.

(19) Paulose, M.; Shankar, K.; Yoriya, S.; Prakasam, H. E.; Varghese, O. K.; Mor, G. K.; Latempa, T. A.; Fitzgerald, A.; Grimes, C. A. Anodic Growth of Highly Ordered TiO_2 Nanotube Arrays to 134 μm in Length. *J. Phys. Chem. B* **2006**, *110*, 16179–16184.

(20) Roy, P.; Berger, S.; Schmuki, P.; TiO_2 Nanotubes: Synthesis and Applications. *Angew. Chem., Int. Ed.* **2011**, *50*, 2904–2939.

(21) William, K. P. Color anodizing of aluminum. U.S. patent, 04060462, **1977**, Nov. 29.

(22) Qi, M.; Lidorikis, E.; Rakich, P. T.; Johnson, S. G.; Joannopoulos, J. D.; Ippen, E. P.; Smith, H. I. A Three-Dimensional Optical Photonic Crystal with Designed Point Defects. *Nature* **2004**, *429*, 538–542.

(23) Canham, L. Handbook of Porous Silicon, Springer International Publishing: Cham, Switzerland, 2014; Chaper 2.

(24) Park, S.; Kim, S.; Park, S.; Lee, W. I.; Lee, C. Effects of Functionalization of TiO2 Nanotube Array Sensors with Pd Nanoparticles on Their Selectivity. *Sensors* **2014**, *14*, 15849–15860.

(25) Lin, S.; Li, D. A Selective Room Temperature Formaldehyde Gas Sensor using TiO_2 nanotube Arrays. *Sens. Actuators, B.* **2011**, *156*, 505–509.

(26) Habisreutinger, S. N.; Schmidt-Mende, L.; Stolarczyk, J. K. Photocatalytic Reduction of CO_2 on TiO_2 and Other Semiconductors. *Angew. Chem., Int. Ed.* **2013**, *52*, 7372–7408.

(27) Linsebigler, A. L.; Lu, G.; Yates Jr, J. T. Photocatalysis on TiO_2 Surfaces: Principles, Mechanisms, and Selected Results. *Chem. Rev.* **1995**, *95*, 735–758.

(28) Wang, J.; Tafen, D. N.; Sewis, J. P.; Hong, Z.; Manivannan, A.; Zhi, M.; Li, M.; Wu, N. Origin of Photocatalytic Activity of Nitrogen-Doped TiO_2 Nanobelts. *J. Am. Chem. Soc.* **2009**, *131*, 12290–12297.

(29) Li, Y.; Sasaki, T.; Shimizu, Y.; Koshizaki, N. Hexagonal-Close-Packed, Hierarchical Amorphous TiO_2 Nanocolumn Arrays: Transferability, Enhanced Photocatalytic Activity, and Superamphiphilicity without UV Irradiation. *J. Am. Chem. Soc.* **2008**, *130*, 14755–14762.

(30) Gouda, L.; Gottesman, R.; Ginsburg, A.; Keller, D. A.; Haltzi, E.; Hu, J.; Tirosh, S.; Anderson, A. Y.; Zaban, A. Open Circuit Potential Build-Up in Perovskite Solar Cells from Dark Conditions to 1 Sun. *J. Phys. Chem. Lett.* **2015**, *6*, 4640–4645.

(31) Qin, P.; Paulose, M.; Dar, M. I.; Moehl, T.; Arora, N.; Gao, P.; Varghese, O. K.; Grätzel, M.; Nazeeruddin, M. K. Stable and Efficient Perovskite Solar Cells Based on Titania Nanotube Arrays. *Small* **2015**, *11*, 5533–5539.

(32) Wang, P.; Zakeeruddin, S. M.; Humphry-Baker, R.; Moser, J. E.; Grätzel, M. Molecular-Scale Interface Engineering of TiO_2 nanocrystals: Improving the Efficiency and Stability of Dye-Sensitized Solar Cells. *Adv. Mater.* **2013**, *15*, 2101–2104.

(33) Park, J.-G.; Kim, S.-H.; Magkiriadou, S.; Choi, T. M.; Kim, Y.-S.; Manoharan, V. Full-Spectrum Photonic Pigments with Non-iridescent Structural Colors through Colloidal Assembly. *Angew. Chem., Int. Ed.* **2014**, *53*, 2899–2903.

(34) Forster, J. D.; Noh, H.; Liew, S. F.; Saranathan, V.; Schreck, C. F.; Yang, L.; Park, J.-G.; Prum, R. O.; Mochrie, S. G. J.; O'Hern, C. S.; Cao, H.; Dufresne, E. R. Biomimetic Isotropic Nanostructures for Structural Coloration. *Adv. Mater.* **2010**, *22*, 2939–2944.

(35) Xiao, M.; Li, Y.; Allen, M. C.; Deheyn, D. D.; Yue, X.; Zhao, J.; Gianneschi, N. C.; Shawkey, M. D.; Dhinojwala, A. Bio-Inspired Structural Colors Produced via Self-Assembly of Synthetic Melanin Nanoparticles. *ACS Nano* **2015**, *9*, 5454–5460.

(36) Kolle, M.; Salgard-Cunha, P. M.; Scherer, M. R. J.; Huang, F.; Vukusic, P.; Mahajan, S.; Baumberg, J. J.; Steiner, U. Mimicking the Colourful Wing Scale Structure of the papilio Blumei Butterfly. *Nat. Nanotechnol.* **2010**, *5*, 511–515.

(37) Coyle, S.; Prakash, G. V.; Baumberg, J. J.; Abdelsalem, M.; Bartlett, P. N. Spherical Micromirrors from Templated Self-Assembly: Polarization Rotation on the Micron Scale. *Appl. Phys. Lett.* **2003**, *83*, 767–769.

(38) Kinoshita, S.; Yoshioka, S.; Structrual Colors in Nature: The Role of Regularity and Irregularity in the Structure. *ChemPhysChem* **2005**, *6*, 1442–1459.

(39) González-Urbina, L.; Baert, K.; Kolaric, B.; Pérez-Moreno, J.; Clays, K. Linear and Nonlinear Optical Properties of Colloidal Photonic Crystals. *Chem. Rev.* **2012**, *112*, 2268– 2285.

(40) Zhu, K.; Neale, N. R.; Miedaner, A.; Frank, A. J. Enhanced Charge-Collection Efficiencies and Light Scattering in Dye-Sensitized Solar Cells Using Oriented TiO_2 Nanotubes Arrays *Nano Lett.* **2007**, *7*, 69–74.

(41) Loewen, E. R.; Popov, E. *Diffraction Gratings and Applications*, CRC Press, New York, USA, **1997.**

(42) Zhang, J.-T.; Wang, L.; Luo, J.; Tikhonov, A.; Kornienko, N.; Asher, S. A. 2-D Array Photonic Crystal Sensing Motif. *J. Am. Chem. Soc*. **2011**, *133*, 9152–9155.

(43) Ye, X.; Li, Y.; Dong, J.; Xiao, J.; Ma, Y.; Qi, L. Facile Synthesis of ZnS Nanobowl Arrays and Their Applications as 2D Photonic Crystal Sensors. *J. Mater. Chem. C* **2013**, *1*, 6112– 6119.

(44) Zhao, Y.; Xie, Z.; Gu, H.; Zhu, C.; Gu, Z. Bio-inspired Variable Structural Color Materials. *Chem. Soc. Rev.* **2012**, *41*, 3297–3317.

(45) Vanmeert, F.; Snickt, G. V.; Janssens, K. Plumbonacrite Identified by X-ray Powder Diffraction Tomography as a Missing Link during Degradation of Red Lead in a Van Gogh Painting. *Angew. Chem., Int. Ed*. **2015**, *54*, 3607–3610.

(46) Kusnetzow, A.; Dukkipati, A.; Babu, K. R.; Singh, D.; Vought, B. W.; Knox, B. E.; Birge, R. R. The Photobleaching Sequence of a Short-Wavelenght Visual Pigment. *Biochemistry* **2001**, *40*, 7832–7844.

(47) Gu, Y.; Zhang, L.; Yang, J. K. W.; Yeo, S. P.; Qiu, C.-W. Color Generation via Subwavelength Plasmonic Nanostructures. *Nanoscale* **2015**, *7*, 6409–6419.

(48) Zhu, X.; Vannahme, C.; Højlund-Nielsen, E.; Mortensen, N. A.; Kristensen, A. Plasmonic Colour Laser Printing. *Nat. Nanotechnol.* **2016**, *11*, 325–329.

Table of Contents

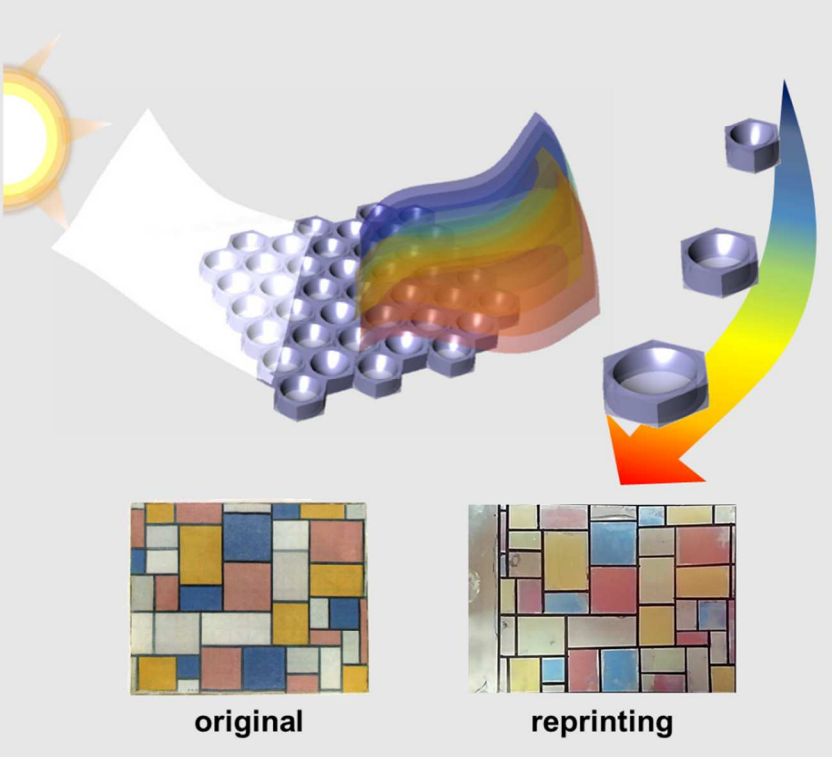

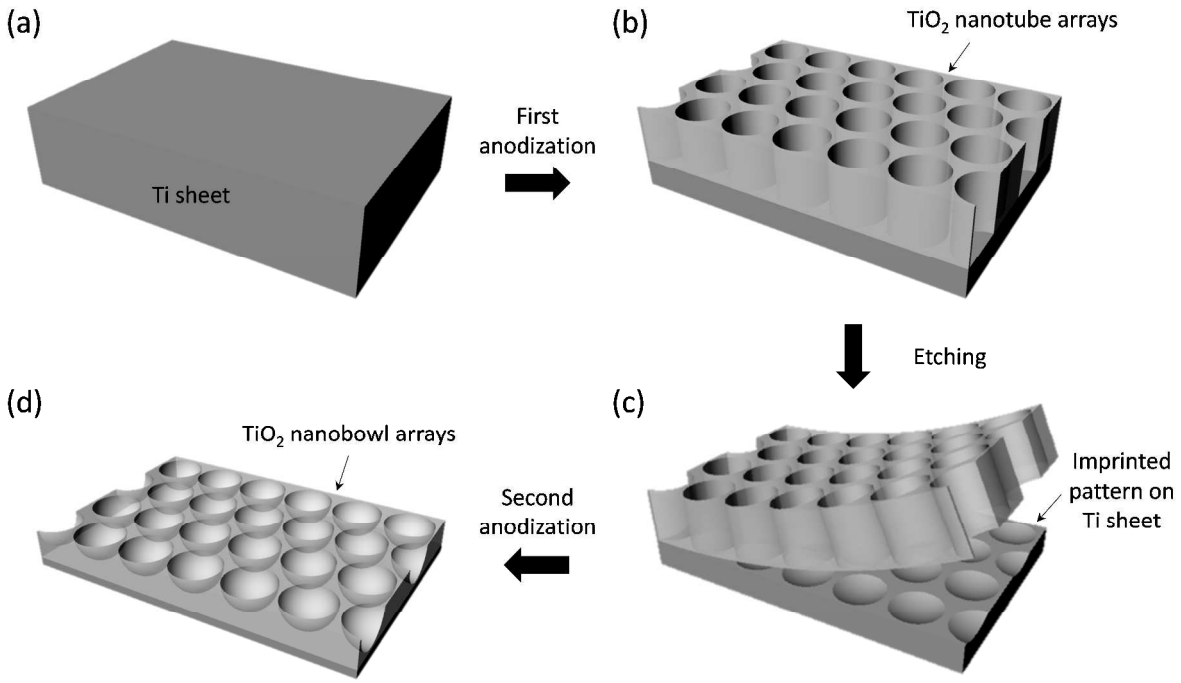

Figure 1. A schematic diagram of the fabrication of TiO_2 nanobowl arrays with a structural color. (a) A Ti sheet was prepared as a source of TiO_2. (b) TiO_2 nanotubes are formed on the Ti sheet through first anodization step. (c) The oxide layer was removed by using a sticky tape and ultrasonication leaving a hexagonal concave pattern on the Ti sheet. (d) TiO_2 nanobowl arrays with a structural color were fabricated by applying anodizing potential for several seconds.

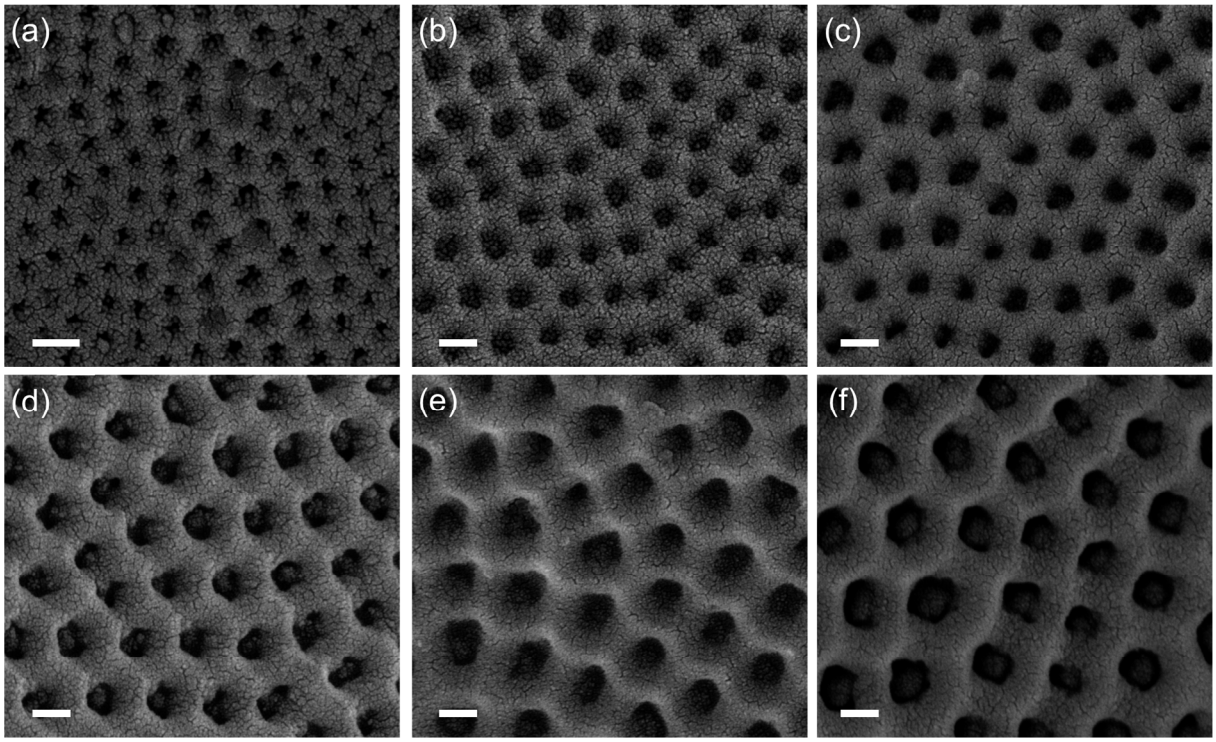

Figure 2. SEM images of TiO_2 nanobowl arrays with different diameters of air cavities that prepared by altering anodizing potential: (a) 30 V, (b) 40 V, (c) 50 V, (d) 60 V, (e) 65 V, and (f) 75 V. Scale bars indicate a length of 100 nm.

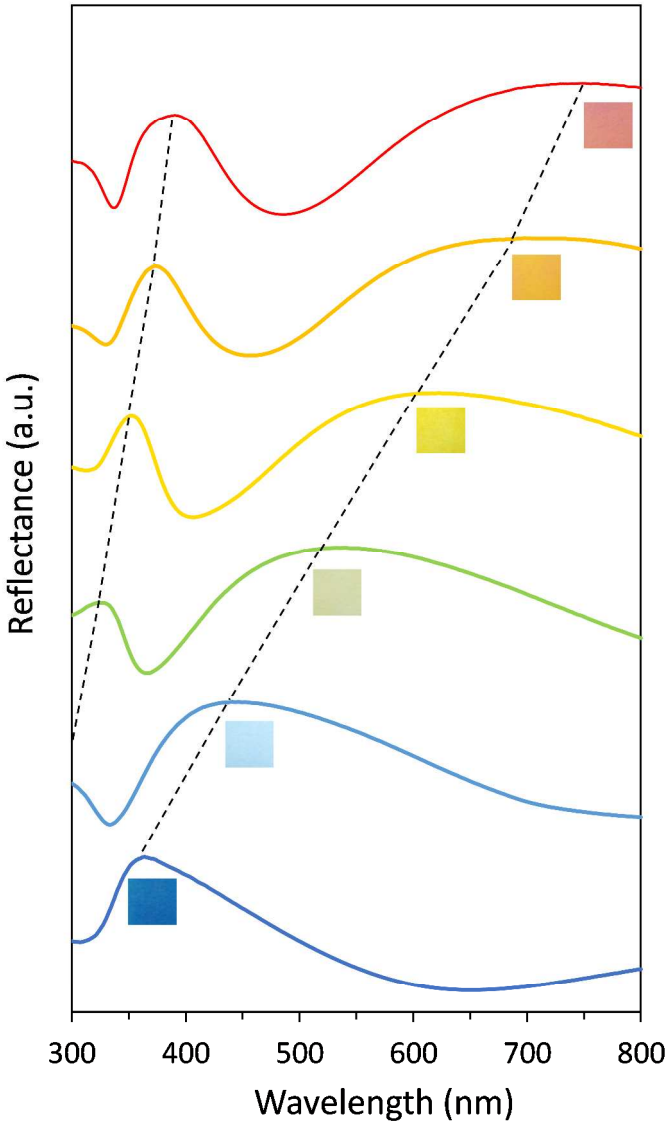

Figure 3. Reflectance spectra of TiO_2 nanobowl arrays with different diameter air cavities. The trend (dotted) lines approximate the shift of the peaks with increasing diameter of the nanostructures.

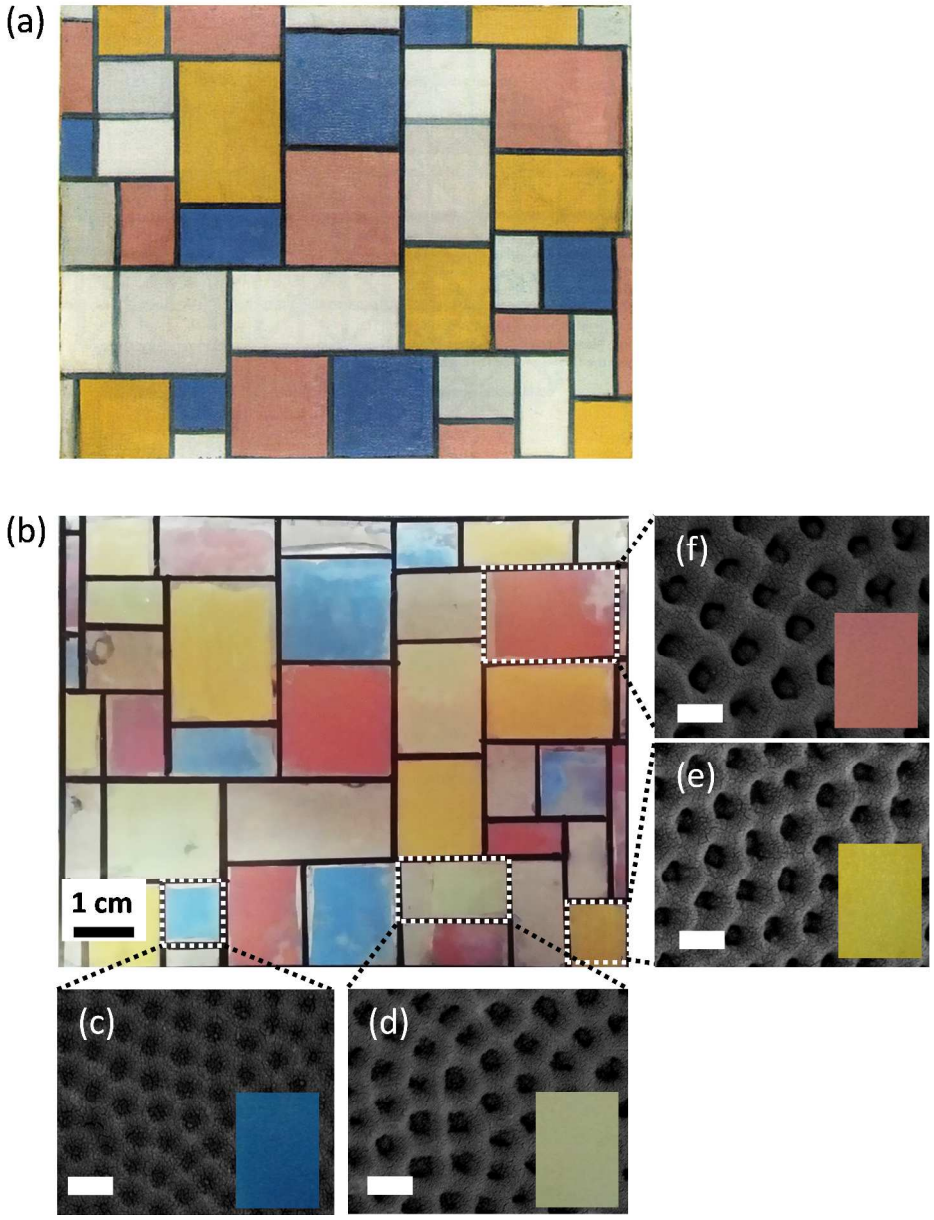

Figure 4. (a) A Mondrian painting known as *Composition with Color Planes and Gray Lines*. (b) The reproduced image on a centimeter scale. (c–f) SEM images of selected areas, which illustrate different diameters and uniform alignment of the nanobowls. White scale bar indicates a length of 200 nm.

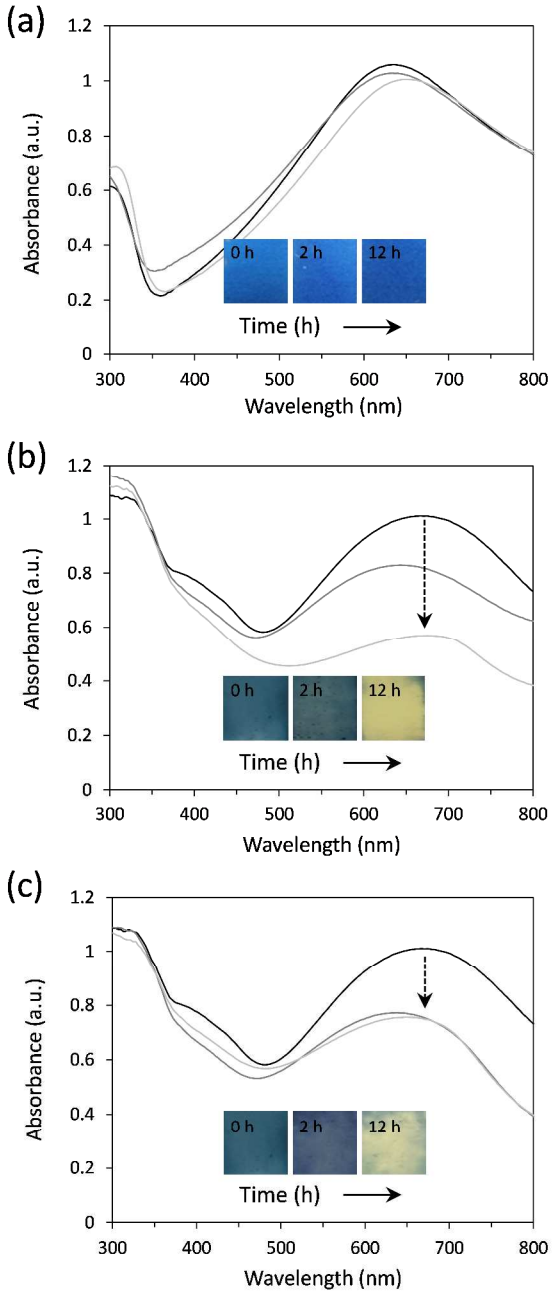

Figure 5. UV-vis absorbance change of (a) TiO_2 nanobowl arrays with a blue color and (b) a N3 dye coated on the P25 under irradiation by direct sunlight, and (c) N3 dye coated on the P25 under irradiation of fluorescent light for 12 h. Insets are images taken during the stability test.

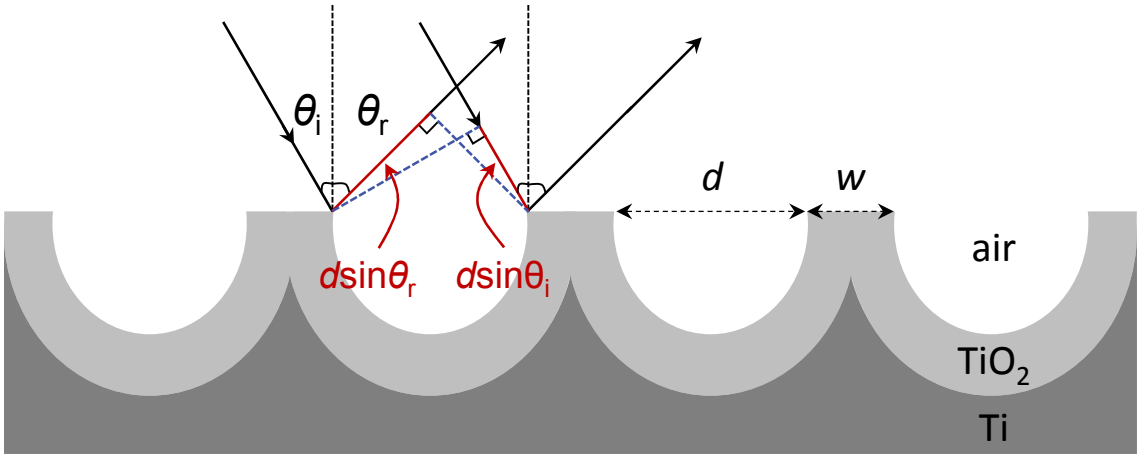

Scheme 1. The reflection path of incident light on the TiO_2 nanobowl structure.

Table 1. Structural Parameters and Reflection Wavelengths of the Synthesized TiO_2 Nanobowl Arrays with Different Colors

Entry	w (nm)	d (nm)	λ_c (nm)[a]	λ_m (nm)[b]
Indigo	35 ± 0.6	41 ± 3.2	325	361 ± 3.2
Blue	47 ± 4.6	52 ± 5.6	432	434 ± 10.2
Green	55 ± 0.6	61 ± 5.1	506	514 ± 11.4
Yellow	61 ± 2.1	83 ± 1.7	600	599 ± 12.4
Orange	66 ± 0.6	92 ± 9.8	654	677 ± 10.1
Red	67 ± 4.6	106 ± 7.8	695	707 ± 9.3

[a] λ_c is the calculated peak wavelength.

[b] λ_m is the measured peak wavelength.